Second Sight A2E16 System Multi-Coil Telemetry Link Electromagnetic Safety Assessment

(07/25/2018)

I. Background

The electromagnetic safety assessment for the A2E16 retinal prosthesis system utilizing a multi-coil telemetry approach is presented in this report. The model used in this report has a cubical voxel resolution of 0.25 mm^3. This report contains a brief introduction to the numerical methods used to compute the electromagnetic fields (D-H FDTD) (with D electric field flux and H magnetic field), relevant retinal prosthesis system parameters including internal and external coils (Tables I and II), as well as details of the model construction and tissue properties utilized (Table III). Two cases are provided in this report to ensure that the worst-case scenario with respect to different possible orientations of the external coil is considered: 1. External coil aligned with the temple arm of the glasses and parallel to the implant's coil; and 2. External coil tangential to the forehead of the head model, with the implant's coil tilted with respect to the external coil. D-H FDTD results are compared with simulations executed with a commercial software (COMSOL) for verification.

II. Method and approach

The D-H Finite Difference Time Domain (D-H FDTD) method is used for the computation of the electromagnetic fields induced in the human head due to the radiating external coil of the considered system [1]. The FDTD method is based on a numerical solution of Maxwell's equations, which is based on central difference approximations of derivatives; this method, introduced first by Yee in 1966, is currently a well-established computational electromagnetics method. In this, explicit solutions to Maxwell's equations are derived through central difference approximations of the time and space derivatives, with fields staggered in space and time so as to create a method that can progress spatially and temporally through the so termed "leapfrog" scheme. The explicit equations are iterated in space and time until steady state is achieved (in the case of sinusoidal excitation).

The computational model is terminated using Perfectly Matched Layers (PML) absorbing boundary conditions to approximate a simulation space of infinite size and, therefore, terminate the computational mesh with a reflectionless material (which is non-physical). Compared to the conventional E-H formulation of the FDTD method, the D-H formulation has the benefit that the PML absorbing layers are independent of the background material. Therefore, although the E-H and D-H formulation are mathematically equivalent, the PML layers used in the D-H algorithms are compatible with model truncations and are easier to implement.

The head model used in the simulations was extracted from 'The visible human project' [2]. The properties of the tissues found in the section of the head were obtained from [3] and are presented in the subsequent section. A voxel resolution of 0.25 mm^3 has been used for the simulations presented in this report. This required downsampling of the original data of the visible human project, which is provided at a resolution of 1 mm.

The multicoil geometry and relative arrangement, in the case of parallel external and implant coils, is illustrated schematically in Figure 1. The radiating structure, which includes two coils (termed “driver” coil and “transmitter” coil), is mounted on glasses worn by the patient, and its arrangement in the computational model is inspired by CAD files of the system provided by Second Sight Medical Products, Inc. The driver coil is connected to the source while the transmitter coil is inductively coupled to the driver coil: the theory behind this arrangement is extensively covered in manuscripts by Kumar and Lazzi [4-6], and will not be repeated here for brevity.

Tables I and II provide the parameters (geometrical and electrical) of the telemetry system employed experimentally and reproduced in the computational model. The driver coil currents in Table II are the experimentally measured, and have been provided by Second Sight Medical Products, Inc, as a function of the distance between external coils and implant coil. Table III provides the tissue properties at the operating frequency of 3.156 MHz [3], which have been used for the results in this report.

In the numerical simulations to compute the SAR, the total current carried by the driver and transmitter coils is forced to specific values, following the procedure detailed in [7, 8]. The amplitude of the current used for the driver coil is derived from the experimentally determined RMS current according to the schedule in Table II; the current used for the transmitter coil is derived from SPICE simulations, with computed coupling coefficients determined using CST and verified by partial inductance method. The electric field is then scaled to match the fields produced by the corresponding current. SARs computed with the D-H FDTD method are verified using COMSOL (Finite-Element Method).

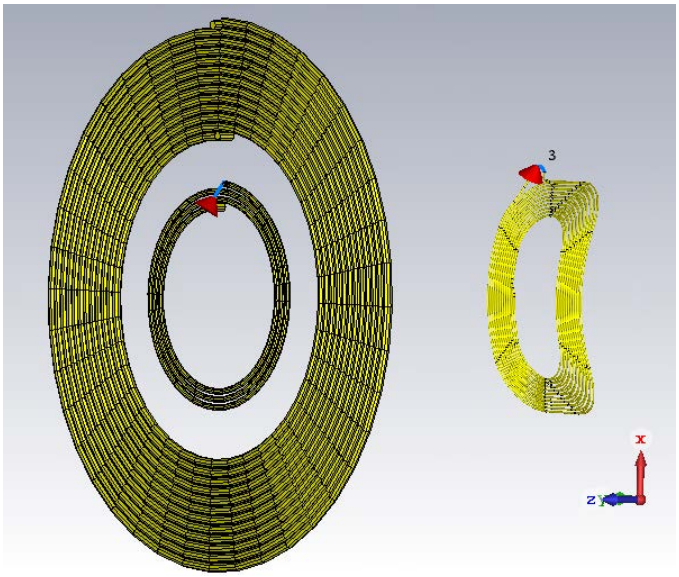

Figure 1. Schematic of the multicoil geometry and relative arrangement, in the case of parallel external and implant coils, employed in the A2E16 retinal prosthesis system.

Table I: Telemetry Coil Parameters (experimental data, provided by Second Sight Medical Products, Inc).

Parameter	Value
Driver Coil Parameters	
Outer diameter	15 mm
Inner diameter	12.03 mm
Number of turns	3
Wire diameter (No Insulation)	0.38 mm (40/46 Litz)
Inductance	350 nH
Transmitter Coil Parameters	
Outer diameter	37.6 mm
Inner diameter	22.07 mm
Number of turns	12
Wire diameter (No Insulation)	0.68 mm (150/46 Litz)
Inductance	4 µH
Implant Coil Parameters	
Outer diameter	16 x 9.6 mm (elliptical)
Number of turns	2 layers, 10 turns each
Inductance	5.5 µH

Table II: Experimentally determined driver coil currents
(RMS Current provided by Second Sight Medical Products Inc).

Range of distance (mm)	RMS Current (A)	Peak Steady-State Current (A) (Calculated From RMS)
11	3.25e-02	4.60E-02
13	3.56e-02	5.03E-02
15	4.07e-02	5.76E-02
18	5.29e-02	7.48E-02
20	5.93e-02	8.39E-02
22	7.10e-02	1.00E-01
24	7.13e-02	1.01E-01
26	7.15e-02	1.01E-01
28	7.11e-02	1.00E-01

Table III: Tissue properties at the frequency of 3.156 MHz

Tissue Name	Conductivity [S/m]	Relative permittivity	Mass Density [Kg/m^3]
Sinus	0	1	1
Cornea	7.90E-01	8.47E+02	1076
Fat	2.60E-02	2.07E+01	920
Mucous Membrane*	2.96E-01	6.12E+02	1102
Muscle	5.70E-01	4.94E+02	1040
Brain White Matter	1.20E-01	2.79E+02	1043
Gland*	6.73E-01	4.76E+02	1028
Blood Vessel*	3.33E-01	1.42E+02	1102
Electronic case**	7.66E6	0	8570
External Coil Enclosure	10E-14	3	1070
Glass Frame	0	8	1550
PCB (FR4)	10E-12	4.4	1850
PCB Coils	5.98E7	0	8940
Implant Coil (Gold)	4.56E+07	0	19320
Imp Coil Insulation***	2.0E-13	3.5	2330

Cerebellum*	2.34E-01	7.97E+02	1045
Bone Cortical*	3.23E-02	8.06E+01	1908
Cartilage	3.07E-01	5.31E+02	1100
Tendon*	3.96E-01	1.26E+02	1142
Skin Dry	6.72E-02	7.30E+02	1010
Brain Grey Matter	1.99E-01	5.54E+02	1039
Lens	4.52E-01	5.63E+02	1100
Eye Sclera	7.29E-01	6.91E+02	1170
Blood	9.89E-01	1.02E+03	1060
Cerebrospinal Fluid*	2.00E+00	1.09E+02	1007
Vitreous Humor	1.50E+00	7.34E+01	1009
Bone Marrow*	5.72E-03	3.04E+01	1029
Bone Cancellous*	1.03E-01	1.44E+02	1178

* These properties are obtained from [2].

**The implant component electronic case is modeled as niobium.

*** The implant coil and cable Insulation are modeled as Silicone Rubber.

III. Transmitter Coil Current

In order to derive the induced current flowing in the transmitter coil that is imposed in the FDTD and COMSOL SAR simulations, we must first compute the coupling coefficient between the driver and transmitter coils. To accomplish this, the coupling coefficients between driver and transmitter coils, K_{12}, and between transmitter and receiver coils, K_{23}, were computed using CST Microwave Studio, and the dominant coupling coefficient, K_{12}, was subsequently validated using the partial inductance method (see Table IV). Next, a SPICE circuit model (Figure 2) incorporating the experimentally determined parameters (inductances, resistances, capacitances), along with the computed coupling coefficients from CST, was used to calculate the current in the transmitter coil. This induced transmitter coil current is then used for all SAR simulations along with the experimentally determined driver coil current.

Table IV: Computed Coupling Coefficient Between Driver and Transmitter Coils (K_{12})

Quantity	Separation Distance	CST Computed Value	Partial Inductance Method Value
K_{12}	**28mm**	0.25	0.26

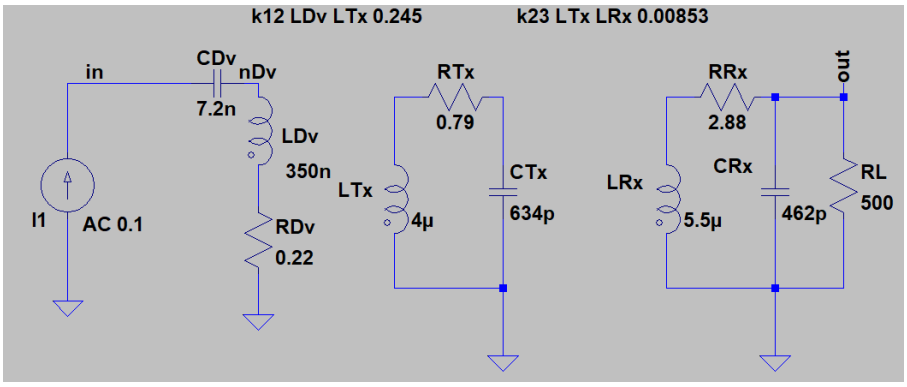

Figure 2. SPICE model of the A2E16 system.

For a separation distance of 28 mm between the external and implant coils and a peak driver current of 100 mA, for example, this approach leads to k_{12}=0.25, k_{23}=0.01 and a current in the transmitter coil of 707

mA. Different configurations/distances can be approached in similar way to determine the current induced in the transmitter coil.

IV. Results: SAR and Current density

In the FDTD method, simulation time and memory requirements were reduced by including in the simulation mesh the section of the model in the proximal region of the transmitter and receiver coils ("truncated" model), while distal regions of the model are embedded into reflectionless absorbing boundary conditions. The boundaries of the truncated model are indicated in Figure 3 with dashed lines. The 0.25 mm resolution computational model is composed of 300 × 300 × 300 computational cells. In the first configuration considered for SAR simulations, the external and implant coils are parallel and have a separation distance of 28 mm. This configuration (parallel coils with external coil at the maximum specified range) represents the worst case scenario since the external coil is adjacent to the human tissue and the current in the driver coil is highest (see Table II, with driver coil current amplitude of 100 mA and transmitter coil current amplitude of 707 mA). Figure 3 shows the computational model in three-dimensions as well as a cross-section of the model on a plane through the center of the coils. SAR and induced current results for this configuration (worst case scenario) are provided in Table V and VI. Both Tables show that IEEE and Canadian (RSS-102) standards safety limits are satisfied with ample margin of safety.

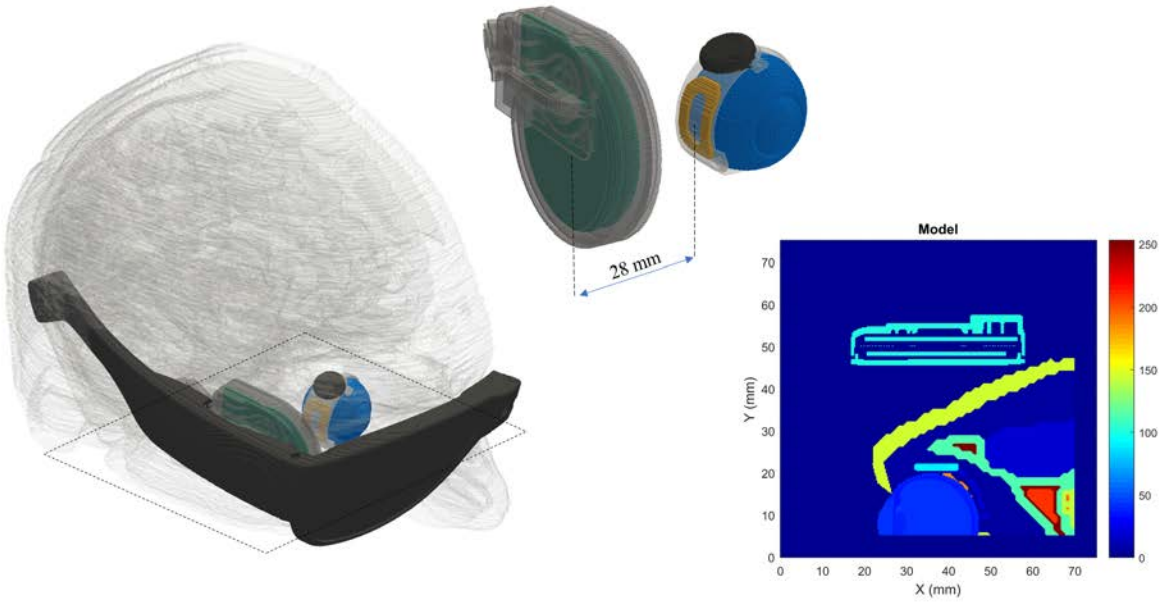

Figure 3. Voxelized computational model used in the FDTD mesh (worst case scenario).

Table V: SAR induced in the human head (worst case scenario)

Quantity	Computed Values (3.156 MHz)	Forward Telemetry Limit (3.156 MHz)	Forward Telemetry Limit (Canada RSS-102) (3.156 MHz)	Conclusion
Maximum averaged 1 gram SAR	**0.006 W/kg**	1.6 W /kg	1.6 W /kg	Passed
Maximum averaged 10 gram SAR	**0.003 W/kg**	2 W/kg	N/A	Passed

Table VI: Maximum current densities induced in the human head (worst case scenario)

Maximum Current density (A/m^2) averaged over 1 cm^2 area	Computed Values (3.156 MHz)	Forward Telemetry Limit (3.156 MHz)	Conclusion
Avg Jx	**0.613 A/m^2**	6.3 A/m^2	Passed
Avg Jy	**0.804 A/m^2**	6.3 A/m^2	Passed
Avg Jz	**1.433 A/m^2**	6.3 A/m^2	Passed

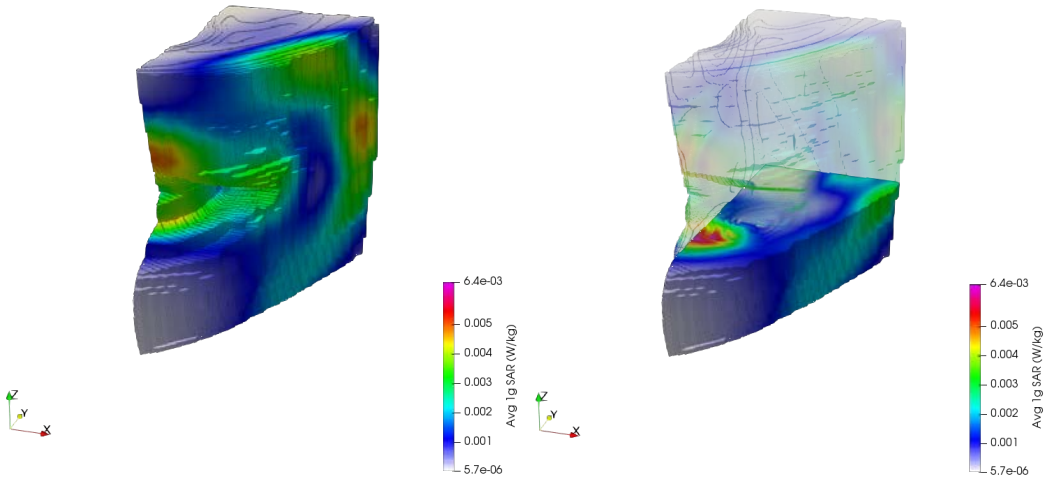

Figure 4. Average 1g SAR (W/kg) for the worst case scenario.

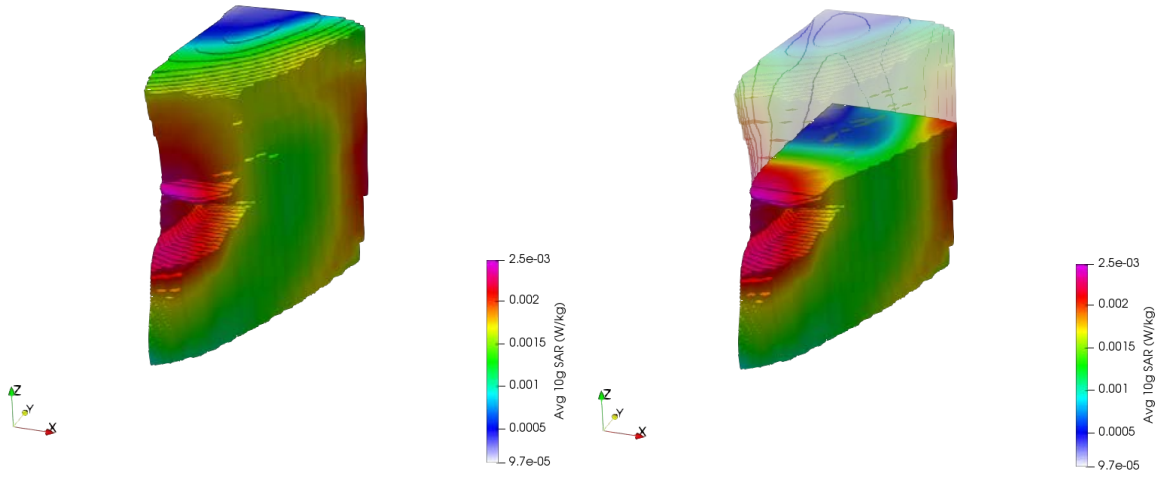

Figure 5. Average 10g SAR (W/kg) for the worst case scenario

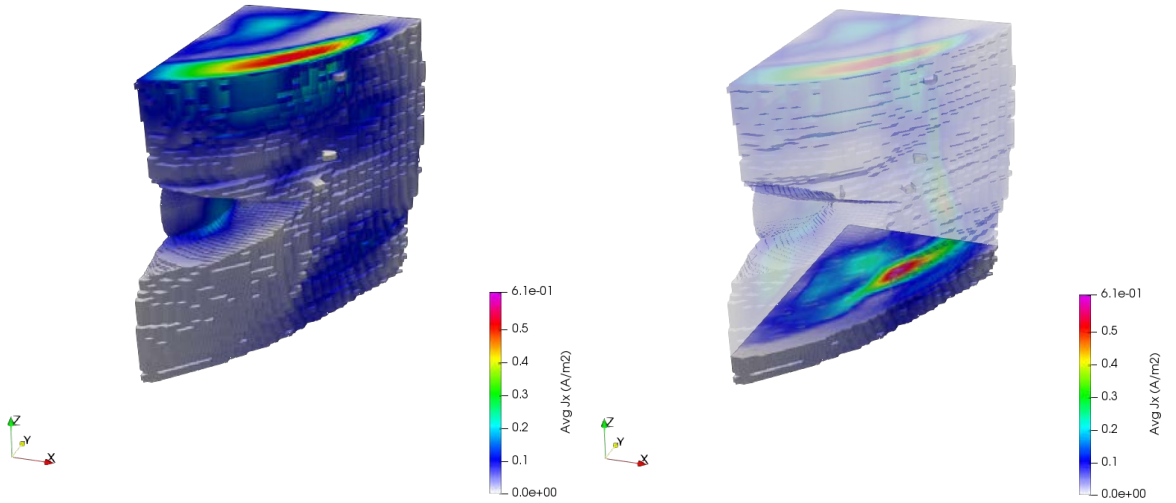

Figure 6. Average (over 1 cm^2) x-directed current density (A/m^2) for the worst case scenario

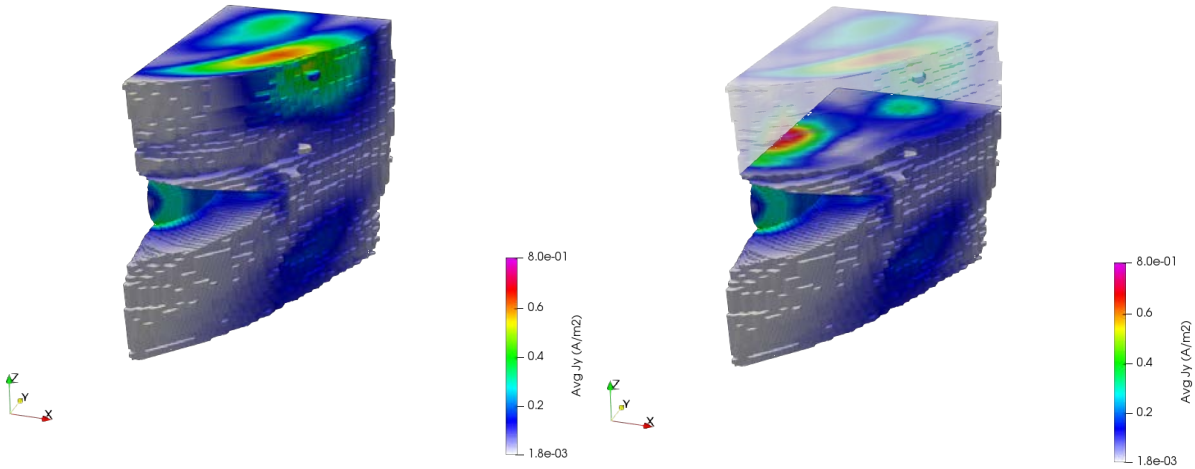

Figure 7. Average (over 1 cm^2) y-directed current density (A/m^2) for the worst case scenario

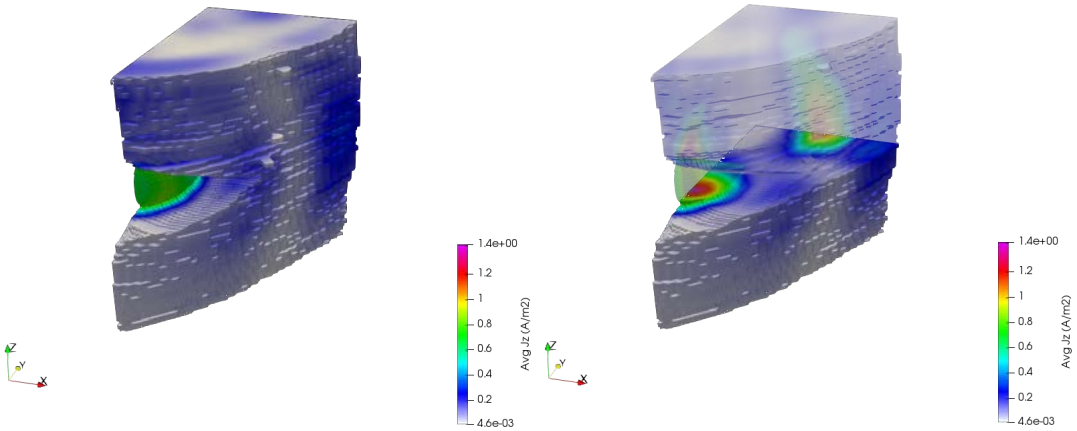

Figure 8. Average (over 1 cm^2) z-directed current density (A/m^2) for the worst case scenario

For completeness, we have also considered the case when the external coil is tangential to the forehead (thus, with a larger surface are in close proximity to the scalp compared to the worst case scenario reported above). In this configuration ("tilted" external coil), the quality of the link between transmitter and implant coil is somewhat degraded, requiring slightly higher transmit currents for a given separation distance. As a result, even though the distance between the external coil and implant coil is reduced, the required driver coil current amplitude (as empirically determined by Second Sight, Inc.) to maintain link quality remains at 100 mA, with a corresponding transmitter coil current amplitude of 707 mA. Figure 9 shows the voxelized model and the boundaries of the truncated model (dashed lines) for this configuration. SAR and induced current results for this configuration ("tilted" case scenario) are provided in Table VII and VIII. Again, both Tables show that safety limit are satisfied with ample margin.

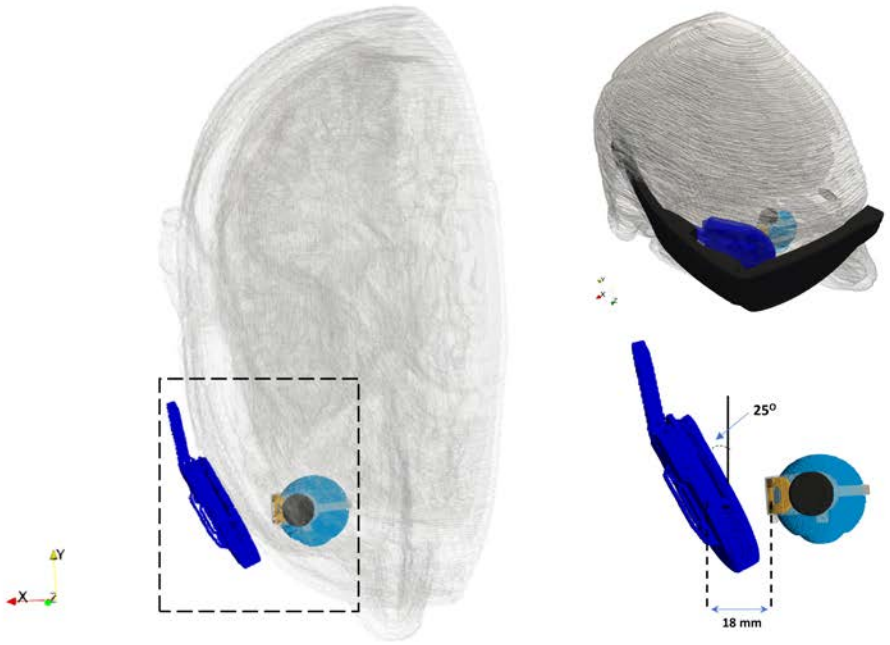

Figure 9. Voxelized computational model used in the FDTD mesh ("tilted" external coil scenario)

Table VII: SAR induced in the human head ("tilted" external coil scenario)

Quantity	Computed Values (3.156 MHz)	Forward Telemetry Limit (3.156 MHz)	Forward Telemetry Limit (Canada RSS-102) (3.156 MHz)	Conclusion
Maximum averaged 1 gram SAR	**0.019 W/kg**	1.6 W /kg	1.6 W /kg	Passed
Maximum averaged 10 gram SAR	**0.008 W/kg**	2 W/kg	N/A	Passed

Table VIII: Maximum current densities induced in the human head ("tilted" external coil scenario)

Maximum Current density (A/m^2) averaged over 1 cm^2 area	Computed Values (3.156 MHz)	Forward Telemetry Limit (3.156 MHz)	Conclusion
Avg Jx	**1.14 A/m^2**	6.3 A/m^2	Passed
Avg Jy	**1.50 A/m^2**	6.3 A/m^2	Passed
Avg Jz	**2.51 A/m^2**	6.3 A/m^2	Passed

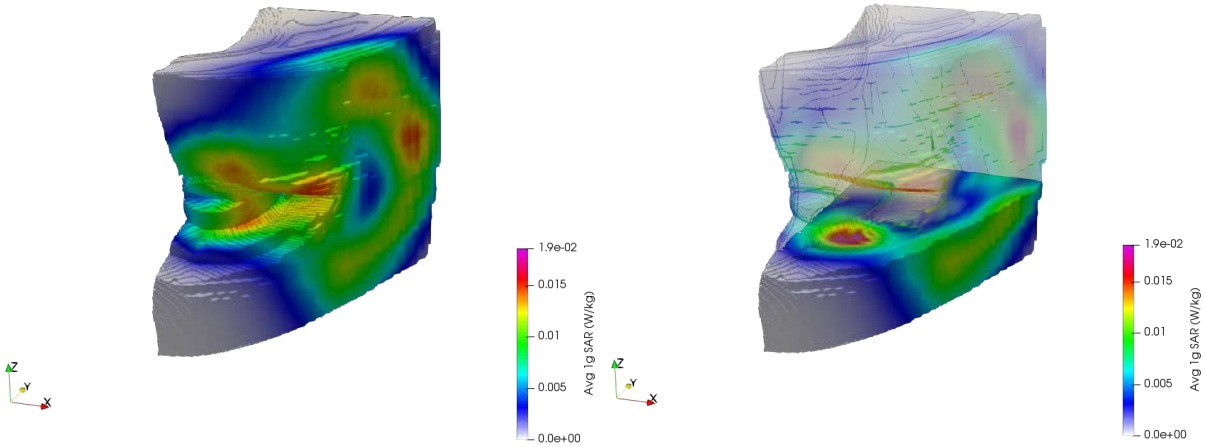

Figure 10. Average 1g SAR (W/kg) for the "tilted" external coil scenario.

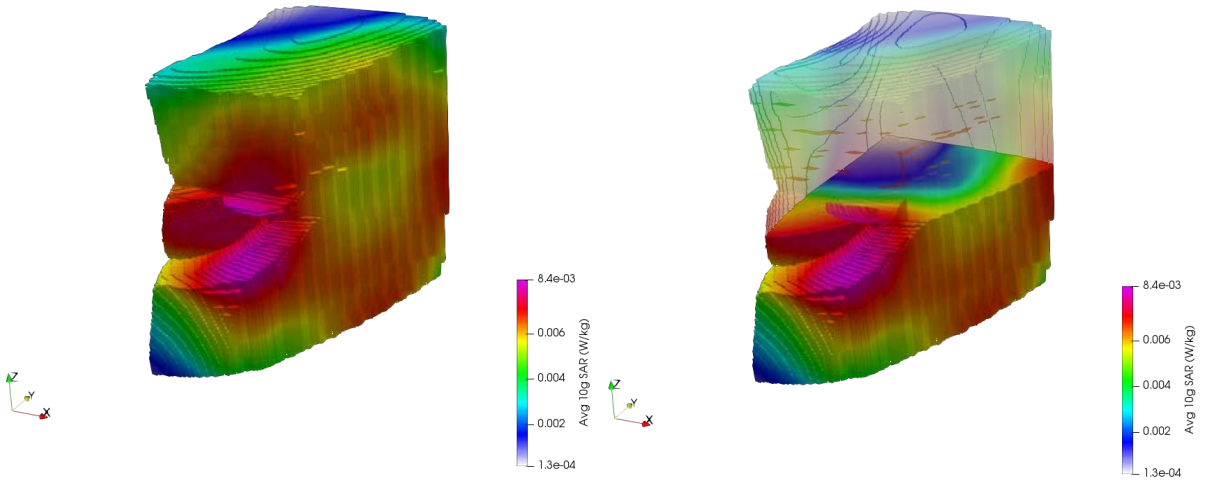

Figure 11. Average 10g SAR (W/kg) for the "tilted" exterrnal coil scenario

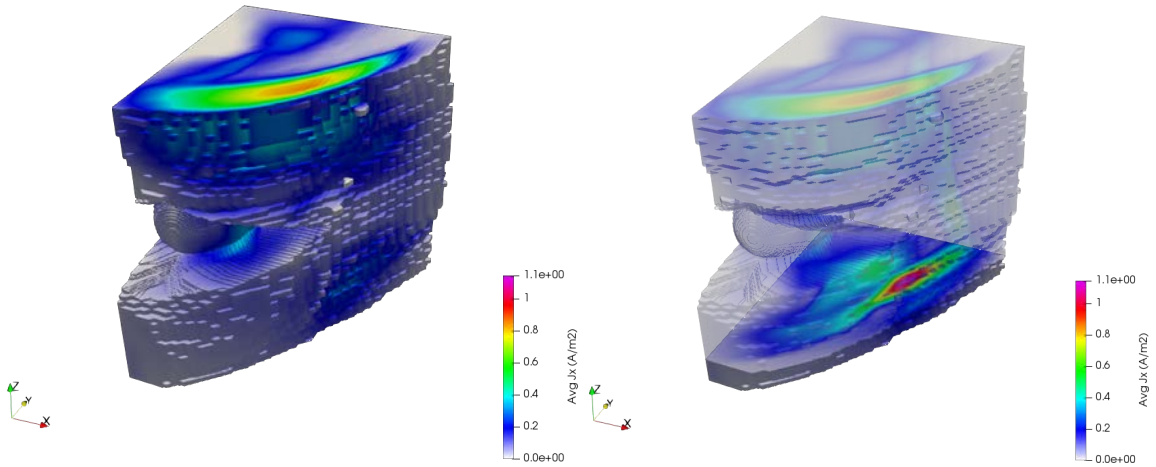

Figure 12. Average (over 1 cm^2) x-directed current density (A/m^2) for the "tilted" external coil scenario

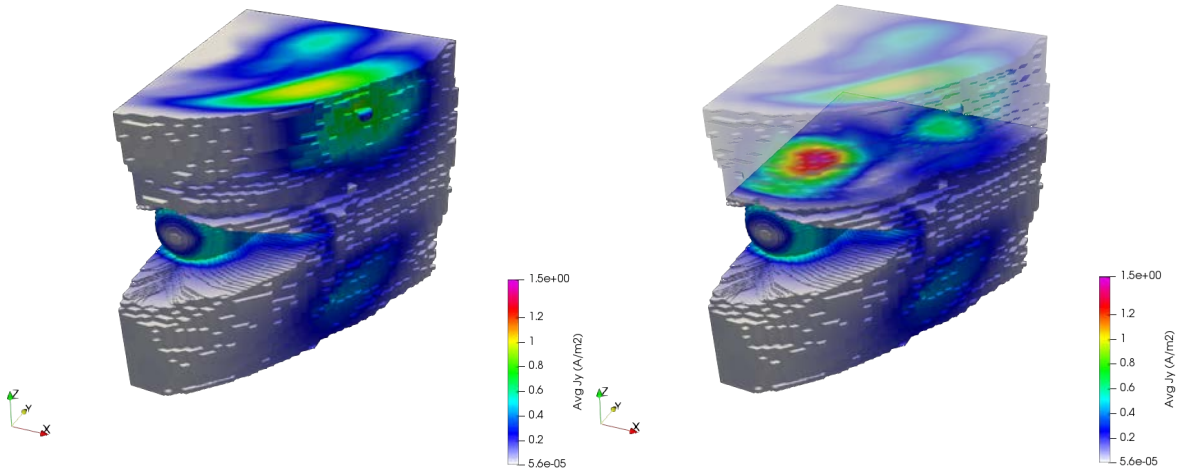

Figure 13. Average (over 1 cm^2) y-directed current density (A/m^2) for the "tilted" external coil scenario

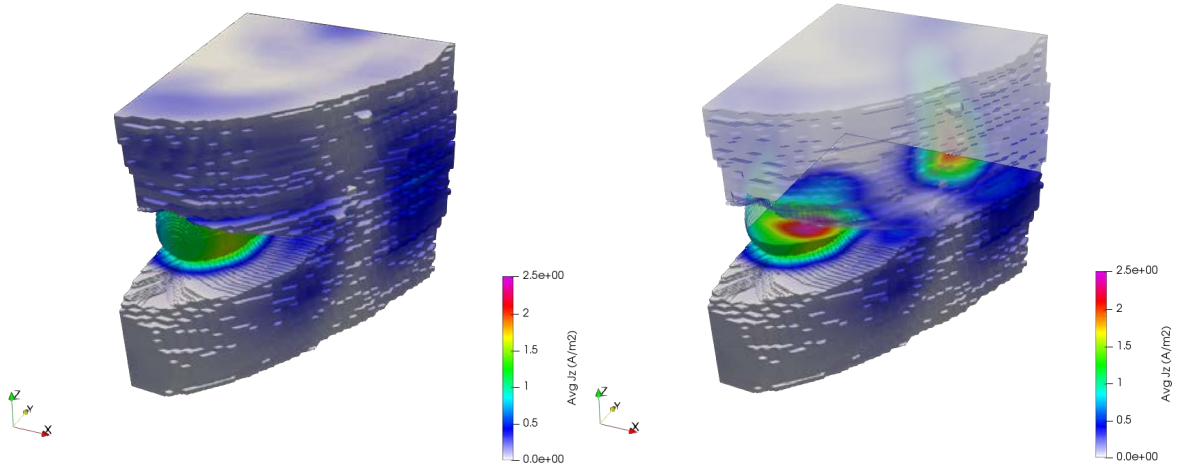

Figure 14. Average (over 1 cm^2) z-directed current density (A/m^2) for the "tilted" external coil scenario

To further validate the FDTD computational results, we used COMSOL Multiphysics (commercial software) to simulate the system and its interaction with the human head. Figure 15 shows the model implemented in COMSOL: the human model is extracted from the National Library of Medicine (NLM) Visible Man Project [4]. The resolution of human head model is coarser compared to the voxelized model used in FDTD simulation, due to the intrinsic limitations of meshing radiating structures and the human head in finite elements. The internal components of the A2E16 multi-coil telemetry system are imported from CAD file formats and incorporated in the head model. Similarly to the FDTD simulations, we assessed averaged SARs and current densities for both parallel coils (28 mm separation distance) and tilted external coil (18 mm separation distance). The COMSOL computational model is shown in Figure 15; tissue properties at 3.156 MHz used in the COMSOL model are given in Table IX. Tables X to XIII compare the FDTD results with the COMSOL results: as shown, the agreement is excellent, with both indicating ample safety margin in all relevant metrics.

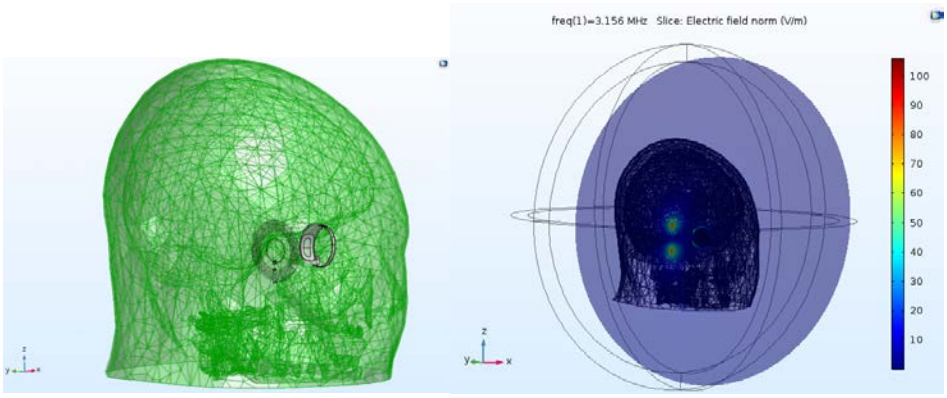

Figure 15. Computational model in COMSOL (worst case scenario configurations)

Table IX: Tissue properties of the COMSOL model at the frequency of 3.156 MHz

Tissue name	Conductivity [S/m]	Relative Permittivity	Mass Density [kg/m3]
Air	0	1	1
Blood	0.98909	1019	1060
Bone Cortical	0.032301	80.563	1908
Brain Grey	0.19897	553.94	1039
Brain White	0.12009	279.43	1043
Cartilage	0.30722	530.47	1100
Cerebellum	0.23357	796.88	1045
Cerebrospinal fluid	2.0002	108.96	1007
Vitreous humor	1.5015	73.411	1009
Fat	0.026023	20.662	920
Skin Dry	0.067159	730.06	1010
Spinal Cord	0.17424	385.06	1075
Teeth	0.032301	80.563	2180
Tongue	0.49796	691.34	1090
Imp Coil Insulation	2.0E-13	3.5	2330
Implant Coil	4.56E+07	0	19320

Table X: SAR induced in the human head for both FDTD and COMSOL (worst case scenario)

Quantity	COMSOL	FDTD	Forward Telemetry Limit (3.156 MHz)	Forward Telemetry Limit (Canada RSS-102) (3.156 MHz)	Conclusion
Maximum averaged 1 gram SAR	**0.005 W/kg**	**0.006 W/kg**	1.6 W /kg	1.6 W /kg	Passed
Maximum averaged 10 gram SAR	**0.002 W/kg**	**0.003 W/kg**	2 W/kg	N/A	Passed

Table XI: Maximum current densities induced in the human head for both FDTD and COMSOL (worst case scenario)

Maximum Current density (A/m^2) averaged over 1 cm^2 area	COMSOL	FDTD	Forward Telemetry Limit	Conclusion
Avg Jx	**0.818 A/m^2**	**0.613 A/m^2**	6.3 A/m^2	Passed
Avg Jy	**0.969 A/m^2**	**0.804 A/m^2**	6.3 A/m^2	Passed
Avg Jz	**1.132 A/m^2**	**1.433 A/m^2**	6.3 A/m^2	Passed

Table XII: SAR induced in the human head for both FDTD and COMSOL ("tilted" external coil scenario)

Quantity	COMSOL	FDTD	Forward Telemetry Limit (3.156 MHz)	Forward Telemetry Limit (Canada RSS-102) (3.156 MHz)	Conclusion
Maximum averaged 1 gram SAR	**0.017 W/kg**	**0.019 W/kg**	1.6 W /kg	1.6 W /kg	Passed
Maximum averaged 10 gram SAR	**0.007 W/kg**	**0.008 W/kg**	2 W/kg	N/A	Passed

Table XIII: Maximum current densities induced in the human head for both FDTD and COMSOL ("tilted" external coil scenario)

Maximum Current density (A/m^2) averaged over 1 cm^2 area	COMSOL	FDTD	Forward Telemetry Limit	Conclusion
Avg Jx	**1.4 A/m^2**	**1.14 A/m^2**	6.3 A/m^2	Passed
Avg Jy	**1.57 A/m^2**	**1.5 A/m^2**	6.3 A/m^2	Passed
Avg Jz	**2.02 A/m^2**	**2.51 A/m^2**	6.3 A/m^2	Passed

References

[1] G. Lazzi, "Unconditionally stable D-H FDTD formulation with anisotropic PML boundary conditions," in *IEEE Microwave and Wireless Components Letters*, vol. 11, no. 4, pp. 149-151, April 2001.

[2] The National Library of Medicine, "The Visible Human Project," 2000. [Online] Available: http://www.nlm.nih.gov/research/visible/

[3] C. Gabriel: Compilation of the dielectric properties of body tissues at RF and microwave frequencies, Report N.AL/OE-TR- 1996-0037, Occupational and environmental health directorate, Radiofrequency Radiation Division, Brooks Air Force Base, Texas (USA), June 1996.

[4] A. Kumar and G. Lazzi, "Multi-Coil Approach to Reduce Electromagnetic Energy Absorption for Wireless Powered Implants," IET Healthcare Technology Letters, vol.1, no.1, pp.21-25, March 2014.

[5] A. Kumar and G. Lazzi, "On the Design of Efficient Multi-coil Telemetry System for Biomedical Implants," IEEE Transaction of Biomedical Circuits and Systems, pp.11-23, 2013

[6] A. Kumar, G. Lazzi, "Multi-coil Telemetry System for Compensation of Coil Misalignment Effects in Implantable Systems," (Invited) IEEE Antenna and Wireless Propagation Letters, Special Cluster on Biomedical Telemetry, pp. 1675- 1678, 2012

[7] V. Singh, A. Roy, R. Castro, K. McClure, J. Weiland, M. Humayun, and G.Lazzi, "Specific Absorption Rate and Current Densities in the Human Eye and Head Induced by the Telemetry Link of a Dual-Unit Epiretinal Prosthesis," IEEE Transactions on Antennas and Propagation, pp.3110-3118, 2009

[8] P. Kosta, J. Paknahad, E. Gamez Rodrıguez, K. Loizos, A. Roy, N. Talbot, S. Seidman, P. Datta, R. Dai, B. Pollack, R. Greenberg, and G. Lazzi, "Electromagnetic Safety Assessment of a Cortical Implant for Vision Restoration," IEEE Journal of Electromagnetics, RF, and Microwaves in Medicine and Biology, pp. 56 – 63, 2018